Bulk metallic glass formation in the (Ti,Zr)–(Ni,Cu)–S system

Oliver Gross[1,2] , **Lucas Ruschel**[1], **Alexander Kuball**[1,2],
Benedikt Bochtler[1,2] , **Bastian Adam**[1] **and Ralf Busch**[1]

[1] Chair of Metallic Materials, Saarland University, Saarbrücken, Germany
[2] Amorphous Metal Solutions GmbH, Homburg, Germany

E-mail: oliver.gross@uni-saarland.de

CrossMark

Abstract

New bulk glass-forming alloy compositions, exceeding a critical casting thickness of 1 mm, are developed in the (quasi-ternary) (Ti,Zr)–(Ni,Cu)–S system. The ternary eutectic composition $Ti_{65.5}Ni_{22.5}Cu_{12}$ is stepwise modified through additions of S (0–8 at%) and Zr (0–22.5 at%) at the expense of Ni and Ti, respectively. By increasing the plate thickness of the casted samples from 500 μm to 1.25 mm, the primary precipitating phases are identified which is for the best glass-formers (e.g. $Ti_{58}Zr_{7.5}Ni_{18.5}Cu_{12}S_4$) an icosahedral phase. In calorimetric experiments, several exothermic crystallization events are observed upon heating glassy samples. The first exothermic event, obscuring the glass transition, is attributed to the formation of the icosahedral phase. As the icosahedral phase forms upon heating and cooling for the best glass-formers, the origin of the increased glass-forming ability might be attributed to a pronounced icosahedral short-range order in the liquid state, impeding the formation of the stable crystalline phases.

Keywords: bulk metallic glass, titanium alloys, sulphur, amorphous metals, industrial applications

(Some figures may appear in colour only in the online journal)

1. Introduction

The formation of metallic glasses is observed in many different alloy systems. A composition is usually termed a bulk metallic glass if its critical casting thickness d_c, which is the thickness up to which fully amorphous samples are obtained, is at least 1 mm. Compositions fulfiling this criterion are found for example in Zr- [1], Ti- [2], Pd- [3], Au- [4], Pt- [5] and Mg-based systems [6]. However, the compositional region, in which bulk glass-formation is observed, is very narrow in many systems and the variation of the alloy composition by a few atomic percent may increase or decrease the glass-forming ability (GFA) significantly [7–9]. The ability of a liquid to form a glass has been attributed to the formation and the extent of local atomic order, termed short-range order (SRO) [10]. The type of SRO varies among the different alloying systems [10, 11] and affects the macroscopic properties of the glass/liquid [12, 13]. A local structural motif that is commonly observed in metallic glass-forming liquids is the icosahedron

[14, 15]. Upon undercooling, the degree of icosahedral short-range order (ISRO) increases [16, 17], which is connected to the viscous slowdown [18, 19] and impedes the formation of the stable crystalline phases [20].

Although the existence of a quasi-crystalline phase points towards ISRO in Ti–Zr–Ni- and the Ti–Zr–Ni–Cu-based liquids [21–23], the GFA is very limited for Ti-rich alloy compositions [21, 24, 25]. Recently, our group reported that S can be an important alloying element, leading to bulk glass formation in various systems and modifying the properties of known compositions beneficially [7, 26, 27]. The addition of S to the (Ti,Zr)–(Ni,Cu) system turned out to effectively increase the GFA [7, 26], resulting in Ti-based BMGs that contain neither toxic (e.g. Be [28]) nor noble (e.g. Pd [2]) elements. The fact that Ni can be completely replaced by Cu makes them promising candidates for biomedical applications [7].

As only a small compositional space in the (Ti,Zr)–(Ni,Cu)–S system has been explored for bulk glass-forming compositions, we chose the ternary eutectic composition

$Ti_{65.5}Ni_{22.5}Cu_{12}$ [29], which is located at higher Ni/Cu concentrations than the previously reported alloys, as a starting point for the alloy development. The addition of S and Zr result in new bulk metallic glass-forming compositions.

2. Experimental

The samples are prepared from high purity elements (Zr 99.99 wt%, Ti 99.999 wt%, Ni 99.98 wt%, Cu 99.999 wt% S 99.995 wt%). Initially, a Ni–S pre-alloy is produced by inductive melting of the pure elements in a fused silica tube under high purity Ar. Subsequently, the pre-alloy is heated with dehydrated B_2O_3 to 1473 K and held at that temperature for at least 6 h. For a more detailed description of the alloying process the reader is referred to [27]. In the next step, the pre-alloy and the other raw elements are alloyed in an arc furnace in a Ti-gettered Ar atmosphere. The homogeneous distribution of the raw elements is guaranteed by flipping and remelting the master alloy at least five times. Amorphous samples are prepared in a custom-built suction casting device where the samples are heated to far above their melting point and sucked into a water-cooled copper mould. The plate shaped moulds with varying thicknesses (0.5, 0.75, 1, 1.25, 1.5 mm) are fed by a gate runner with a diameter of 2 mm (see Results section). As the cooling rate of the plate shaped samples is the lowest in the centre, the samples are ground to half of their initial thickness with an accuracy of ± 50 µm. Subsequently, the ground surface is analysed by x-ray diffraction using a PAN-alytical Empyrean XRD with monochromatic Cu Kα radiation. Calorimetric measurements are performed with a Perkin Elmer DSC8000 using Al pans and a NETZSCH STA 449 Jupiter differential thermal analyser using Y_2O_3 coated graphite crucibles at a rate of 0.333 K s^{-1} under a constant flow of high-purity Ar.

3. Results

The ternary eutectic composition $Ti_{65.5}Ni_{22.5}Cu_{12}$ [29] (blue circle in figure 1) is chosen as a starting point since glass-forming alloy compositions are often located in the vicinity of a deep eutectic. However, this 'rule' should not be considered as limitation if a system is screened for bulk glass-forming composition as certain exceptions exist. An example is the shown in the pseudo-ternary phase diagram in figure 1, the $Ti_{60}Zr_{15}Ni_{12}Cu_5S_8$ [26] bulk glass-forming compositions which is not located close to an eutectic composition [30]. In this study, the element Ni is chosen to be substituted by S since a significant Ni-release might limit the application of the alloy compositions as biomaterial. The compositional shift in the pseudo-ternary (Ti,Zr)–(Ni,Cu)–S phase diagram is visualized as a blue arrow in figure 1.

Figure 2 shows the XRD data for the samples where S is substituted at the expense of Ni to the ternary eutectic composition. At the eutectic composition, three different crystalline phases are in equilibrium, namely the Ti_2Cu, Ti_2Ni and TiNi intermetallic phases [29]. For a more detailed description of the crystalline phases in the Ti–Cu–Ni system under equilibrium conditions, the interested reader is referred to [29]. The
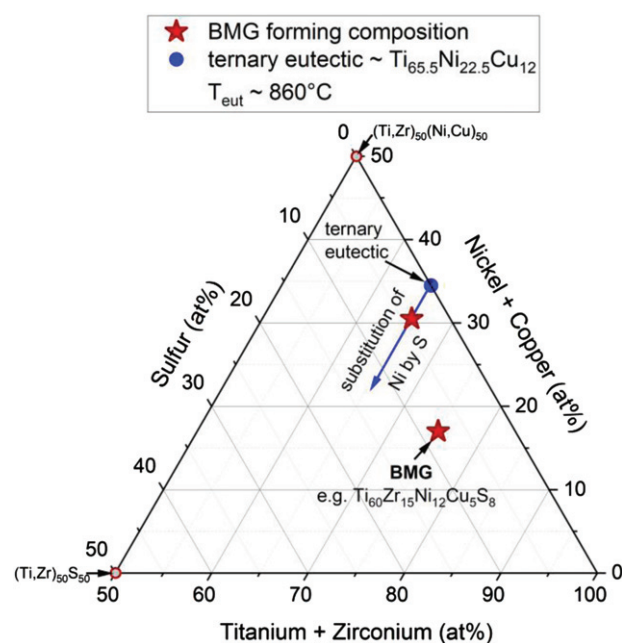

Figure 1. Pseudo-ternary (Ti,Zr)–(Ni,Cu)–S phase diagram. Starting from the ternary eutectic composition, Ni is stepwise substituted by S (blue arrow). The data of the ternary eutectic are taken from [29], whereas the BMG forming composition $Ti_{60}Zr_{15}Ni_{12}Cu_5S_8$ is taken from [26].
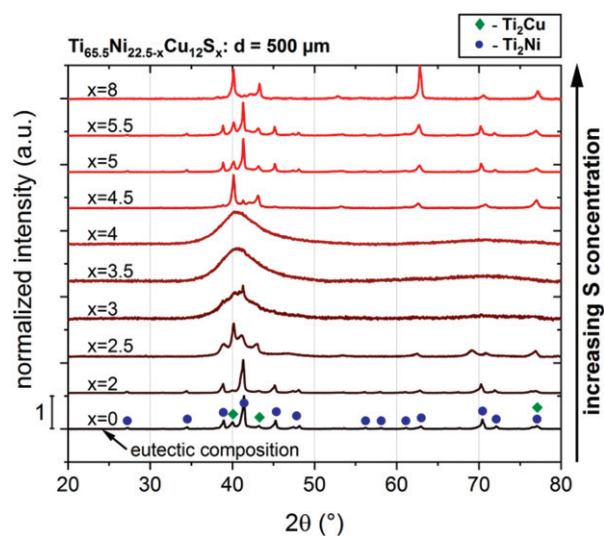
Figure 2. XRD patterns of plate shaped samples with a thickness of 500 µm. Ni is stepwise substituted by S. X-ray amorphous samples are obtained for S concentrations of 3.5 and 4 at%. For reasons of comparison, the XRD patterns are normalized to their maximum intensity value.

Bragg peaks in figure 2 are most probably attributed to the phase Ti_2Cu and Ti_2Ni. However, the TiNi phase might also be present in a smaller volume fraction and/or the Bragg peaks overlap as the non-equilibrium conditions of the casting process lead to a supersaturation of the phases causing a shift of the peak position. Despite the exact phase distribution in the eutectic alloy, the addition of S destabilizes the competing crystalline phases, leading to x-ray amorphous samples at 3.5
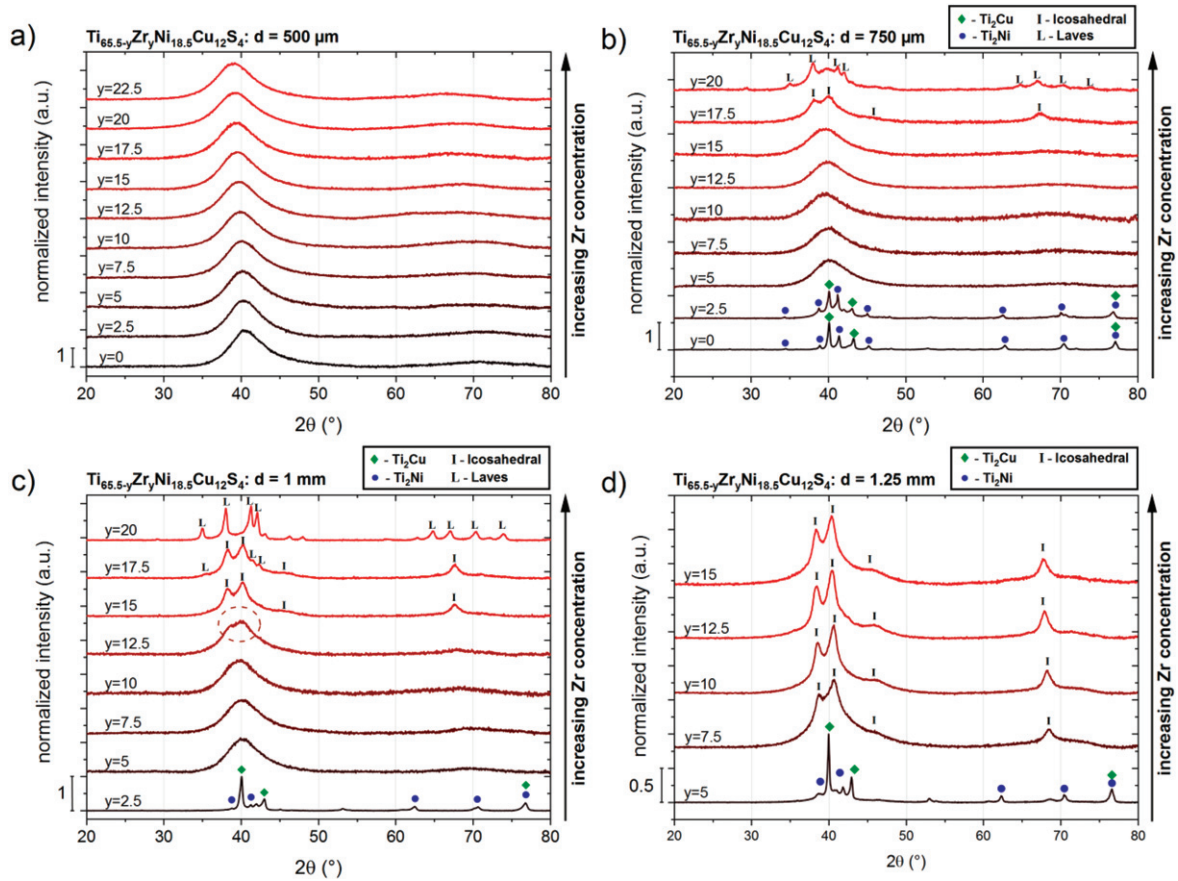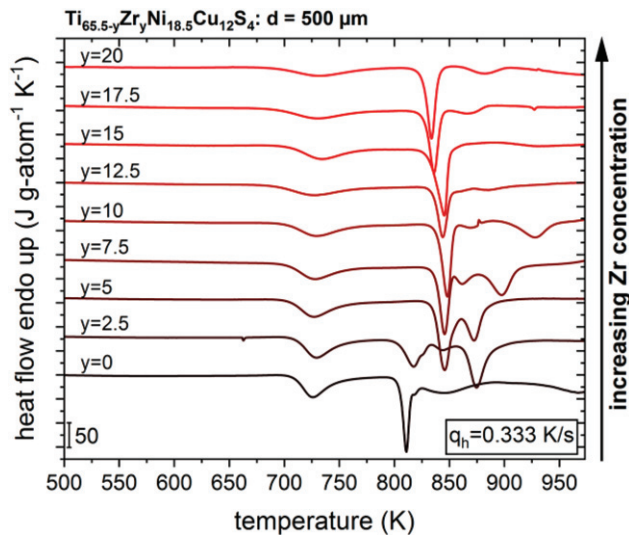
Figure 3. (a)–(d) Show XRD patterns of plate shaped samples with a thickness of 0.5, 0.75, 1 and 1.25 mm. Ti is stepwise replaced by Zr. The glass-forming region narrows with increasing sample diameter and the phases formed due to the decreasing cooling rate are indicated. In (a), the peak maximum of the amorphous halo shifts to lower scattering angles for increasing Zr-content. In (c), the dashed circle at the XRD pattern of the sample containing 12.5 at% Zr indicates that a small fraction of the icosahedral phase might already be present. For reasons of comparison, the XRD pattern are normalized to their maximum intensity value.

and 4 at% S. Lower and higher S-contents result in partially or fully crystalline samples. In [7], a maximum GFA is observed for a S concentration of 8 at% in the same alloying system, but for a different (Ti,Zr)–(Ni,Cu) ratio (see figure 1). For that reason, a sample with the alloy composition $Ti_{65.5}Ni_{14.5}Cu_{12}S_8$ is prepared, exhibiting a fully crystalline character as can be seen from the diffractogram in figure 2. For the further alloy development, the alloy composition with 4 at% S is chosen. In our previous study, the addition of Zr for Ti showed a positive effect on the GFA [26] and Zr is therefore chosen as additional alloying element. In order to evaluate that Zr does not deteriorate the GFA, the 500 μm thick plates are prepared with a Zr content ranging from 2.5 to 22.5 at%. The XRD results are depicted in figure 3(a), showing that all diffractograms exhibit the typical shape observed for x-ray amorphous samples. A clear shift of the peak maximum of the amorphous halo to smaller scattering angles is observed, which is reasonable as Zr possesses a larger atomic diameter than Ti [31] thereby increasing the average atomic distances. The DSC traces of the 500 μm samples are shown in figure 4. For none of the alloy compositions, a glass transition is observed in the calorimetric signal (for a detailed view the reader is referred to figure 6(a)).

The primary exothermic peak, whose minimum is located at approximately 725 K, smears out with increasing Zr-content and is reminiscent of the primary crystallization event observed in Al-based metallic glasses [32, 33]. The position and the extent of the following exothermic events change with composition. If the plate diameter is increased from 500 to 750 μm, the samples with a Zr-content of 5–15 at% remain x-ray amorphous (figure 3(b)). At a Zr concentration of 2.5 at% the Ti_2Ni and Ti_2Cu form, whereas the diffraction pattern of the sample containing 17.5 at% Zr suggests the formation of an icosahedral phase which has been reported in different Ti-based alloys [21, 34, 35]. At a slightly higher Zr concentration (20 at%), the Bragg peaks indicate the presence of the C14 Laves phase which has also been observed in literature [21, 36]. By increasing the sample diameter to 1 mm (figure 3(c)), the glass-forming region further narrows to a compositional range between 5 and 10 at% Zr, and the icosahedral phase is detected for Zr-contents of 12.5 and 15 at%. The XRD pattern of a 1 mm sample containing 17.5 at% Zr now exhibits both signatures, that of the icosahedral and that of the Laves phase. As soon as the sample diameter increase to 1.25 mm (figure 3(d)), the XRD pattern do not show the typical halo
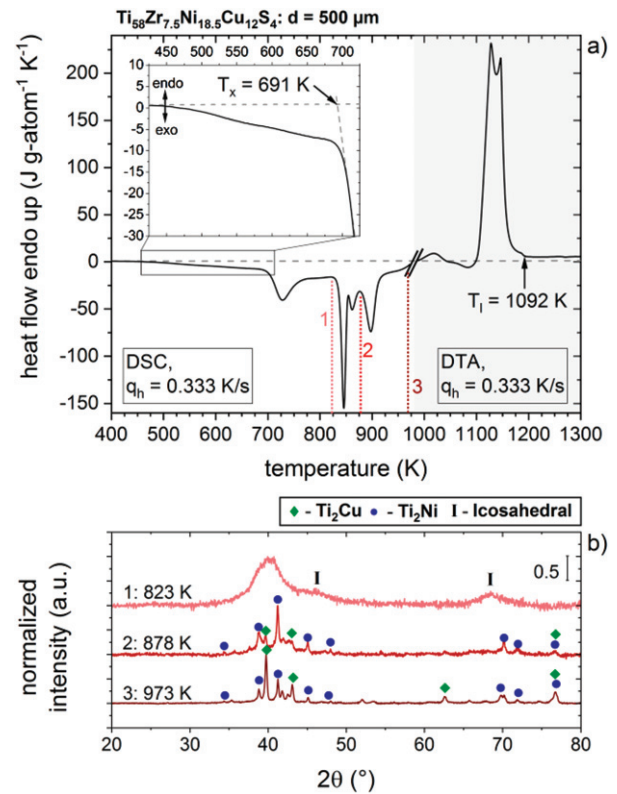
Figure 4. Thermograms of plate shaped samples with a thickness of 500 μm. Ti is stepwise substituted by Zr. The samples were shown to be x-ray amorphous prior all measurements. The curves are shifted vertically for clarity.
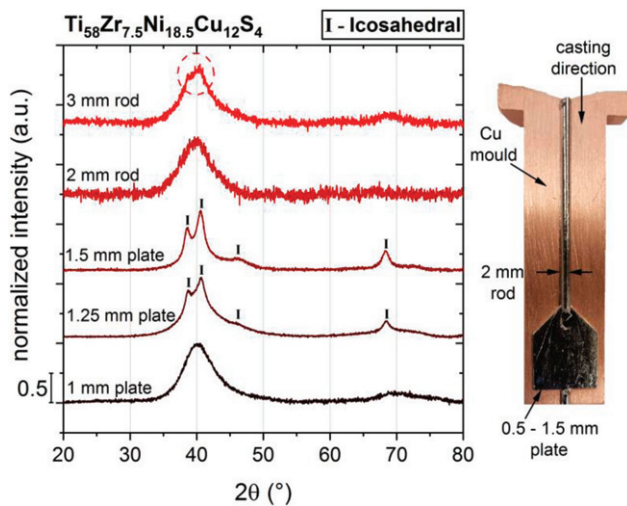
Figure 5. XRD patterns of the $Ti_{58}Zr_{7.5}Ni_{18.5}Cu_{12}S_4$ samples with different geometries. As the cooling rate is lower in plate shaped moulds, the $Ti_{58}Zr_{7.5}Ni_{18.5}Cu_{12}S_4$ alloy composition can be vitrified in cylindrical moulds with a diameter of roughly 3 mm. First signs of the presences of the icosahedral phase can be observed in XRD pattern of the 3 mm rod sample as indicated by the dashed circle. The picture on the right shows the sample geometry used for the determination of the critical casting thickness.

Figure 6. (a) Thermogram of the $Ti_{58}Zr_{7.5}Ni_{18.5}Cu_{12}S_4$ alloy composition. In the temperature range from 400 to 973 K the sample was measured in a DSC and above 973 K the thermogram results from a DTA measurement. The inset in (a) magnifies the low temperature region, showing the exothermic α-relaxation followed by the primary crystallization event at $T_x = 691$ K obscuring the glass transition event. The liquidus temperature T_l is located at 1092 K. The vertical dashed lines labelled with 1, 2, 3 refer to the temperatures to which samples were heated at a rate of 0.333 K s^{-1} and subsequently cooled at 3 K s^{-1}. The XRD patterns of the samples are shown in (b) and the phases formed during the thermal treatment are indicated.

of an amorphous sample for any composition and the icosahedral phase forms in the compositional range above 5 at% Zr.

It should be noted that the critical casting thickness determined from the plate shaped samples is smaller than the values obtained from cylindrical samples. This is due to the smaller cooling rate at the centre of the plates. The effect of the different sample geometries on the critical casting thickness is shown for the $Ti_{58}Zr_{7.5}Ni_{18.5}Cu_{12}S_4$ alloy composition in figure 5. Beside the XRD patterns in figure 5, a typical

sample used for the determination of the critical casting thickness is depicted. The XRD pattern of the plate shaped samples with a diameter of 1.25 and 1.5 mm clearly show signatures that are attributed to the icosahedral phase. In contrast, a cylindrical sample with a diameter of 2 mm exhibits an amorphous XRD pattern. At a sample diameter of 3 mm, the sharpening of the amorphous halo indicates the onset of the formation of the icosahedral phase. Consequently, the critical casting thickness of the $Ti_{58}Zr_{7.5}Ni_{18.5}Cu_{12}S_4$ liquid is roughly 3 mm for cylindrical samples.

In order to investigate the crystallization sequence upon heating from the glassy state, the $Ti_{58}Zr_{7.5}Ni_{18.5}Cu_{12}S_4$ alloy composition is heated in the DSC at 0.333 K s^{-1} to 823 K, 878 K and 973 K. To conserve the structural state of the samples after the thermal treatment, they are rapidly cooled at 3 K s^{-1}. As a temperature reference, the DSC scan of the $Ti_{58}Zr_{7.5}Ni_{18.5}Cu_{12}S_4$ bulk metallic glass up to 973 K is shown in figure 6(a) and the temperatures of the thermal treatments are indicated as dashed lines. The inset in figure 6(a) magnifies the low temperature region, revealing that no step-like event in the heat-flow signal is detected, which would

be attributed to the glass transition. The preceding exothermic event, which starts at ~450 K, is commonly observed in bulk metallic glasses and is most probably attributed to the α-relaxation process. The primary, exothermic crystallization signature, which is connected to the formation of the icosahedral phase (see diffractogram in figure 6(b) at 823 K), obscures the glass transition. At temperatures above the secondary crystallization event (878 K), the icosahedral phase and the remaining glassy phase transform into the Ti_2Ni and the Ti_2Cu phases (figure 6(b)). The last crystallization event seems to solely change the volume ratio between the intermetallic phases (figure 6(b)). Above 973 K, a DTA measurement is shown in figure 6(a). The liquidus temperature is located at 1092 K which is approximately 40 K lower than the eutectic temperature of the $Ti_{65.5}Ni_{22.5}Cu_{12}$ alloy [29].

4. Discussion

The addition of 3.5 and 4 at% of S to the ternary eutectic composition $Ti_{65.5}Ni_{22.5}Cu_{12}$ [29] at the expense of Ni increase the GFA to 500 μm. Interestingly, an S concentration of 8 at%, which was found to be the ideal S-content in the $Ti_{75}Ni_{25-x}S_x$ type of alloys [7], results in fully crystalline samples. As shown in figure 1, so far two different glass-forming regions are identified in the (Ti,Zr)–(Ni,Cu)–S system. The reduction of the ideal S concentration to ~4 at% seems to be a consequence of the increased Ni and Cu content. Consistently to previous observations [7, 26], the substitution of Ti by Zr effectively increase the GFA. As summarized in figure 7, the critical casting thickness for plate shaped samples is 1 mm for Zr concentrations ranging from 5 to 10 at%. These alloy compositions can be considered as bulk metallic glass-forming alloys. The compositional range in which bulk glass formation is observed probably extends to higher Zr-contents for cylindrical samples. As the Zr concentration is only roughly varied in this compositional region, even higher critical casting thickness may be reached at compositions in-between those depicted in figure 7. Minor compositional changes can significantly increase the GFA as shown for Ni-based alloys by Na *et al* [8].

The origin of the increasing GFA through the addition of Zr might be connected to the fact that the primary precipitating phase changes from Ti_2Ni/Ti_2Cu for the Zr-free and Zr-lean alloy compositions to the icosahedral phase for higher Zr-contents. The preferential formation of the icosahedral phase in the compositional range from 5 to 15 at% Zr could be attributed to an increasing ISRO in the liquid phase. A pronounced ISRO reduces the interfacial energy between the liquid and the icosahedral phase [37]. This in turn results in a decreasing energy barrier for the formation of an icosahedral nucleus as the interfacial energy contributes to the power of three to the nucleation barrier. In contrast, a high interfacial energy is considered to be an decisive factor for the GFA in Pt–P-based bulk glass-forming liquids [38, 39]. Although the small interfacial energy is not beneficial for the GFA, the formation of ISRO is expected to increases the melt viscosity [40, 41]. Sluggish atomic movements due to a high viscosity affect the nucleation and growth rate and may lead to
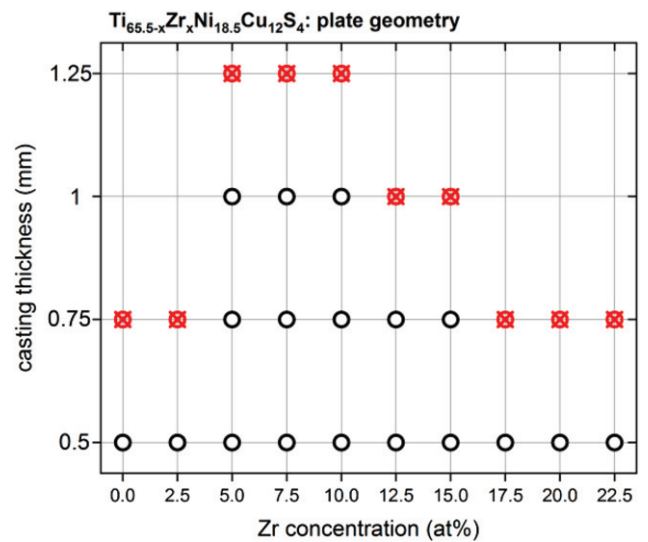
Figure 7. Critical casting thickness for plate shaped samples as a function of the Zr-content. The open, black symbols represent x-ray amorphous samples. The crossed circles are used if a crystalline or quasi-crystalline phase is present in the sample.

an increasing GFA as demonstrated by Na *et al* for Fe-based bulk glass-forming liquids [42]. The importance of the viscosity for the glass formation in this system is supported by the observation that the viscosity at the liquidus temperature of the $Ti_{60}Zr_{15}Cu_{17}S_8$ bulk glass-forming alloy composition (same alloy family as $Ti_{58}Zr_{7.5}Ni_{18.5}Cu_{12}S_4$) is approximately one order of magnitude higher than that of the $Ti_{37}Zr_{42}Ni_{21}$ liquid [22, 30]. As the $Ti_{37}Zr_{42}Ni_{21}$ liquid, which is not a bulk glass-former, also forms the icosahedral phase as primary phase and possess the same T_1 as $Ti_{58}Zr_{7.5}Ni_{18.5}Cu_{12}S_4$ [37], the role of S for the GFA should not be underestimated. The small atomic size of S in comparison to the other alloying elements [31] might further improve the packing density in the liquid state and thereby increase the viscosity of the liquid resulting in an enhanced GFA.

At higher Zr concentrations the primary phase changes from the icosahedral to the Laves phase. This is in agreement with the pseudo-ternary Ti–Zr–(Cu,Ni) phase diagram depicted in [36], suggesting the formation of the Laves phase at ~20 at% Zr for a Ti content of ~65 at%. At a Zr concentration of 17.5 at% and a plate thickness of 1 mm the transition from the icosahedral to the Laves phase is observed. Within this context it should be noted that Kurtuldu *et al* recently reported that bulk glass-forming liquids may form the icosahedral phase as intermediate phase upon cooling form the equilibrium liquid [43]. This metastable intermediate phase primarily nucleates due to the low nucleation barrier resulting from the low interfacial energy and subsequently transforms into the stable phase. This crystallization scenario from the equilibrium liquid cannot be excluded for the type of alloys under investigation, which means that the icosahedral phase might always be the primary phase. However, the clarification of the exact crystallization sequence requires further experiments.

In contrast, the observation of crystallization process upon heating from the glassy state is less challenging due to much

slower dynamics. The results for the $Ti_{58}Zr_{7.5}Ni_{18.5}Cu_{12}S_4$ composition in figure 6 show that the icosahedral phase forms as primary phase and that this crystallization event obscures the glass transition. Consequently, the low degree of atomic mobility close to the glass transition seems sufficient to form the icosahedral phase, suggesting that the structure of the glass is already close to that of the icosahedral phase. A similar crystallization signature concealing the glass transition is observed in Al-based metallic glasses. Due to the extremely high Al-content in these glasses only little atomic mobility is needed to form the fcc Al solid solution [44, 45]. Consequently, the compositional and structural proximity of the glassy phase to the primary precipitating phase provokes the primary exothermic event before reaching the glass transition in both alloy families. The glassy state might be stabilized upon heating by increasing the Cu content which was shown to extend the supercooled liquid region in the $Ti_{75}Ni_{17-z}Cu_zS_8$ type of alloys [7].

5. Conclusion

In summary, it is shown that further bulk glass-forming alloy compositions at higher Ni/Cu concentrations can be found in the pseudo-ternary (Ti,Zr)–(Ni,Cu)–S system. The optimum S-content around the $Ti_{65.5}Ni_{22.5}Cu_{12}$ eutectic composition is located at approximately 4 at% leading to an increase of the glass-forming ability to 500 μm. The addition of 7.5 at% Zr at the expense of Ti increase the critical casting thickness to 1 mm for plate shaped and to roughly 3 mm for cylindrical samples. The glass-forming ability of the $Ti_{58}Zr_{7.5}Ni_{18.5}Cu_{12}S_4$ alloy composition is limited by the nucleation of the icosahedral phase which also forms upon heating from the glassy phase and obscures the glass transition event. These observations suggest the existence of a pounced icosahedral short-range order in the liquid state which might be the origin of the enhanced glass-forming ability through increasing the melt viscosity. Even higher critical casting thickness might be obtained by reducing the step-size of compositional variations on the Ti–Zr axis or by re-adjusting the S-content at a fixed Zr concentration. Moreover, an increase of the Cu concentration might stabilize the glassy phase and retard the formation of the icosahedral phase upon heating.

Acknowledgments

ORCID iDs

Oliver Gross https://orcid.org/0000-0003-4281-6182
Benedikt Bochtler https://orcid.org/0000-0003-0494-735X

References

[1] Peker A and Johnson W L 1993 A highly processable metallic glass: Zr41.2Ti13.8 Cu 12.5Ni10.0Be22.5 *Appl. Phys. Lett.* **63** 2342–4

[2] Zhu S L, Wang X M, Qin F X and Inoue A 2007 A new Ti-based bulk glassy alloy with potential for biomedical application *Mater. Sci. Eng.* A **459** 233–7

[3] Nishiyama N, Takenaka K, Miura H, Saidoh N, Zeng Y and Inoue A 2012 The world's biggest glassy alloy ever made *Intermetallics* **30** 19–24

[4] Schroers J, Lohwongwatana B, Johnson W L and Peker A 2005 Gold based bulk metallic glass *Appl. Phys. Lett.* **87** 404–6

[5] Zhang T and Inoue A 2003 Bulk glassy alloys with low liquidus temperature in Pt-Cu-P system *Mater. Trans.* **44** 1143–6

[6] Zheng Q, Xu J and Ma E 2007 High glass-forming ability correlated with fragility of Mg-Cu(Ag)-Gd alloys *J. Appl. Phys.* **102** 113519

[7] Kuball A, Gross O, Bochtler B, Adam B, Ruschel L, Zamanzade M and Busch R 2019 Development and characterization of titanium-based bulk metallic glasses *J. Alloys Compd.* **790** 337–46

[8] Na J H, Demetriou M D, Floyd M, Hoff A, Garrett G R and Johnson W L 2014 Compositional landscape for glass formation in metal alloys *Proc. Natl Acad. Sci.* **111** 9031–6

[9] Gross O, Eisenbart M, Schmitt L-Y, Neuber N, Ciftci L, Klotz U E, Busch R and Gallino I 2018 Development of novel 18-karat, premium-white gold bulk metallic glasses with improved tarnishing resistance *Mater. Des.* **140** 495–504

[10] Sheng H W, Luo W K, Alamgir F M, Bai J M and Ma E 2006 Atomic packing and short-to-medium-range order in metallic glasses *Nature* **439** 419–25

[11] Gaskell P H 1978 A new structural model for transition metal–metalloid glasses *Nature* **276** 484–5

[12] Ding J, Cheng Y Q, Sheng H and Ma E 2012 Short-range structural signature of excess specific heat and fragility of metallic-glass-forming supercooled liquids *Phys. Rev.* B **85** 1–5

[13] Gross O, Neuber N, Kuball A, Bochtler B, Hechler S, Frey M and Busch R 2019 Signatures of structural differences in Pt–P- and Pd–P-based bulk glass-forming liquids *Commun. Phys.* **2** 83

[14] Hirata A, Kang L J, Fujita T, Klumov B, Matsue K, Kotani M, Yavari A R and Chen M W 2013 Geometric frustration of icosahedron in metallic glasses *Science* **341** 376–9

[15] Hirata A, Guan P, Fujita T, Hirotsu Y, Inoue A, Yavari A R, Sakurai T and Chen M 2011 Direct observation of local atomic order in a metallic glass *Nat. Mater.* **10** 28–33

[16] Ding J and Ma E 2017 Computational modeling sheds light on structural evolution in metallic glasses and supercooled liquids *npj Comput. Mater.* **3** 9

[17] Schenk T, Holland-Moritz D, Simonet V, Bellissent R and Herlach D M 2002 Icosahedral short-range order in deeply undercooled metallic melts *Phys. Rev. Lett.* **89** 1–4

[18] Hao S G, Wang C Z, Li M Z, Napolitano R E and Ho K M 2011 Dynamic arrest and glass formation induced by self-aggregation of icosahedral clusters in Zr1−xCux alloys *Phys. Rev.* B **84** 064203

[19] Cheng Y Q, Sheng H W and Ma E 2008 Relationship between structure, dynamics, and mechanical properties in metallic glass-forming alloys *Phys. Rev.* B **78** 1–7

[20] Herlach D M 1994 Non-equilibrium solidification of undercooled metallic metals *Mater. Sci. Eng.* R **12** 177–272

[21] Wang L, Ma L, Ma C and Inoue A 2003 Formations of amorphous and quasicrystal phases in Ti-Zr-Ni-Cu alloys *J. Alloys Compd.* **361** 234–40

[22] Hyers R W, Bradshaw R C, Rogers J R, Rathz T J, Lee G W, Gangopadhyay A K and Kelton K F 2004 Surface tension and viscosity of quasicrystal-forming Ti–Zr–Ni alloys *Int. J. Thermophys.* **25** 1155–62

[23] Molokanov V V and Chebotnikov V N 1990 Quasicrystals and amorphous alloys in Ti-Zr-Ni system: Glassforming ability, structure and properties *J. Non-Cryst. Solids* **117–118** 789–92

[24] Molokanov V V and Chebotnikov V N 1990 Glass forming ability, structure and properties of Ti and Zr-intermetallic compound based alloys *Mech. Corros. Prop.* A **40–41** 319–31

[25] Wang Y-L and Xu J 2008 Ti (Zr)-Cu-Ni bulk metallic glasses with optimal glass-forming ability and their compressive properties *Metall. Mater. Trans.* A **39** 2990–7

[26] Kuball A, Gross O, Bochtler B and Busch R 2018 Sulfur-bearing metallic glasses: A new family of bulk glass-forming alloys *Scr. Mater.* **146** 73–6

[27] Kuball A, Bochtler B, Gross O, Pacheco V, Stolpe M, Hechler S and Busch R 2018 On the bulk glass formation in the ternary Pd-Ni-S system *Acta Mater.* **158** 13–22

[28] Duan G, Wiest A, Lind M L, Kahl A and Johnson W L 2008 Lightweight Ti-based bulk metallic glasses excluding late transition metals *Scr. Mater.* **58** 465–8

[29] Schuster J C and Cacciamani G Cu–Ni–Ti (Copper–Nickel–Titanium) *Light Metal Systems. Part 4*, ed G Effenberg and S Ilyenko (Berlin: Springer) pp 1–18

[30] Kuball A 2019 *Development, Characterization and Processing of a Novel Family of Bulk Metallic Glasses: Sulfur-Containing Bulk Metallic Glasses* (Saarbrücken: Saarland University)

[31] Laws K J, Miracle D B and Ferry M 2015 A predictive structural model for bulk metallic glasses *Nat. Commun.* **6** 8123

[32] Liao J P, Yang B J, Zhang Y, Lu W Y, Gu X J and Wang J Q 2015 Evaluation of glass formation and critical casting diameter in Al-based metallic glasses *Mater. Des.* **88** 222–6

[33] Kuball A, Stolpe M and Busch R 2018 Crystallization behavior of the Al86Ni8Y6 metallic glass forming alloy upon rapid cooling *J. Alloys Compd.* **737** 398–404

[34] Kelton K F, Kim W J and Stroud R M 1997 A stable Ti-based quasicrystal *Appl. Phys. Lett.* **70** 3230–2

[35] Yang Q B 1988 Structures of Ti 2 (Ni, V) in crystalline and quasicrystalline phases *Philos. Mag. Lett.* **57** 171–6

[36] Lin X H and Johnson W L 1995 Formation of Ti-Zr-Cu-Ni bulk metallic glasses *J. Appl. Phys.* **78** 6514–9

[37] Lee G W, Gangopadhyay A K, Croat T K, Rathz T J, Hyers R W, Rogers J R and Kelton K F 2005 Link between liquid structure and the nucleation barrier for icosahedral quasicrystal, polytetrahedral, and simple crystalline phases in Ti-Zr-Ni alloys: Verification of Fank's hypothesis *Phys. Rev.* B **72** 174107

[38] Gross O, Riegler S S, Stolpe M, Bochtler B, Kuball A, Hechler S, Busch R and Gallino I 2017 On the high glass-forming ability of Pt-Cu-Ni/Co-P-based liquids *Acta Mater.* **141** 109–19

[39] Legg B A, Schroers J and Busch R 2007 Thermodynamics, kinetics, and crystallization of Pt57.3Cu14.6Ni5.3P22.8 bulk metallic glass *Acta Mater.* **55** 1109–16

[40] Busch R, Schroers J and Wang W H 2007 Thermodynamics and Kinetics of Bulk Metallic Glass *MRS Bull.* **32** 620–3

[41] Mukherjee S, Schroers J, Johnson W L and Rhim W-K 2005 influence of kinetic and thermodynamic factors on the glass-forming ability of zirconium-based bulk amorphous alloys *Phys. Rev. Lett.* **94** 245501

[42] Na J H, Demetriou M D and Johnson W L 2011 Fragility of iron-based glasses *Appl. Phys. Lett.* **99** 161902

[43] Kurtuldu G, Shamlaye K F and Löffler J F 2018 Metastable quasicrystal-induced nucleation in a bulk glass-forming liquid *Proc. Natl Acad. Sci.* **115** 6123–8

[44] Kim W T, Gogebakan M and Cantor B 1997 Heat treatment of amorphous Al85Y5Ni10 and Al85Y10Ni5 alloys *Mater. Sci. Eng.* A **226–228** 178–82

[45] Wilde G, Wu R I and Perepezko J H 2001 Nanocrystallization of Al-rich metallic glasses *Advances in Solid State Physics 40* vol 287 (Berlin: Springer) pp 391–405